THEORETICAL ANALYSIS FOR STUDYING THE FRETTING WEAR PROBLEM OF STEAM GENERATOR TUBES IN A NUCLEAR POWER PLANT

CHOON YEOL LEE*, YOUNG SUCK CHAI, and JOON WOO BAE
School of Mechanical Engineering
Yeungnam University
214-1 Dae-dong, Gyongsan-si, Korea, 712-749
*To whom correspondence should be addressed. cylee@yu.ac.kr

Received August 11, 2004
Accepted for Publication January 10, 2005

Fretting, which is a special type of wear, is defined as small amplitude relative motion along the contacting interface between two materials. The structural integrity of steam generators in nuclear power plants is very much dependent upon the fretting wear characteristics of Inconel 690 U-tubes. In this study, a finite element model that can simulate fretting wear on the secondary side of the steam generator was developed and used for a quantitative investigation of the fretting wear phenomenon. Finite element modeling of elastic contact wear problems was performed to demonstrate the feasibility of applying the finite element method to fretting wear problems. The elastic beam problem, with existing solutions, is treated as a numerical example. By introducing a control parameter *s*, which scaled up the wear constant and scaled down the cycle numbers, the algorithm was shown to greatly reduce the time required for the analysis. The work rate model was adopted in the wear model. In the three-dimensional finite element analysis, a quarterly symmetric model was used to simulate cross tubes contacting at right angles. The wear constant of Inconel 690 in the work rate model was taken as $K=26.7\times10^{-15}\ Pa^{-1}$ from experimental data obtained using a fretting wear test rig with a piezoelectric actuator. The analyses revealed donut-shaped wear along the contacting boundary, which is a typical feature of fretting wear.

KEYWORDS : Fretting Wear, Finite Element Analysis, Work Rate Model, Wear Depth, Contact Pressure

1. INTRODUCTION

It is generally believed that failure accidents in industrial facilities and structures are caused by wear and/or fatigue of the loaded elements. In contrast with the numerous active, long-term studies on failures due to high-temperature fatigue, corrosive fatigue, and fretting fatigue, only a relatively small number of studies on fretting wear have been performed.

Fretting, which is a special type of wear, is characterized as small amplitude oscillation along the contacting interface between two materials [1]. Since Eden et al. [2] first reported on this phenomenon, which was termed "fretting" by Tomlinson [3], considerable effort has been directed towards elucidating this type of behavior. Waterhouse [4] classified the fretting phenomenon into three categories: fretting wear, fretting fatigue, and fretting corrosion. Other works [5-11] have provided some important general fretting theories or experimental results for fretting wear and/or fretting fatigue. Recently, Vingsbo and Soderberg [9] classified fretting wear into four types: stick, mixed stick/slip, gross slip, and sliding. Ko [8] and Fisher et al. [10, 11] investigated the wear constant experimentally by studying fretting wear of tube materials for a steam generator in a nuclear power plant. In Korea, most fretting wear studies have concentrated on experimentally determining the wear constants for materials in nuclear power plants, such as Inconel or Zircalloy tubes [12-16].

Although most fretting wear studies have been carried out experimentally, some theoretical approaches have also been attempted. Mackin et al. [17] studied the effects of surface roughness on the wear properties of the interface between fiber and titanium-aluminum matrix composite materials. Strömberg [18] studied a two-dimensional contact wear problem between a punch and a plate to obtain wear depth and normal contact pressure distributions using a theoretical wear formulation via an augmented Lagrangian method.

Typical factors that affect fretting wear include the normal contact force, amplitude of the excitation distance,

excitation frequency, and environmental factors such as the contact type or the state of the surface. Archard [19] proposed a theoretical model that was capable of computing the wear volume. Fisher et al. [10, 11] suggested a work rate model to predict the remaining lifetime of a steam generator tube affected by fretting wear. The work rate model related the time rate change in the amount of energy dissipated by fretting wear, i.e., the time rate change of the normal force components for the total sliding distance, with the wear rate, as follows

$$\dot{W} = \frac{1}{t}\int F_n \cdot ds \tag{1}$$

$$\dot{V} = K\dot{W} \tag{2}$$

where $\dot{W}$ is the rate change of the dissipated energy, $\dot{V}$ is the wear rate, F_n is the normal force, s is the total sliding distance, and K is defined as the wear constant with units of Pa^{-1}. For our research, we chose to follow the recent trend of using the wear constant defined in the work rate model to calculate the amount of fretting wear.

In this study, a finite element model that can simulate fretting wear on the secondary side of the steam generator, which arises from flow-induced vibrations (FIV) of the U-tubes or foreign objects, was developed in order to investigate the behavior of the fretting wear phenomenon quantitatively. Finite element modeling of elastic contact wear problems was performed to demonstrate the feasibility of applying the finite element method to fretting wear problems in consideration of frictional contact. A numerical example treated is the elastic beam problem, which has existing solutions by Strömberg [18]. By introducing a control parameter s, which scaled up the wear constant and scaled down the cycle numbers, the algorithm was shown to greatly reduce the time required for the analysis. In the wear model, the work rate model was adopted. The results of the analyses behaved in a similar qualitative manner with the previous solutions by Strömberg [18].

In the three-dimensional finite element analysis, a quarterly symmetric model was used to simulate tubes contacting at right angles. The wear constant of Inconel 690 in the work rate model was taken as K=26.7 $\times 10^{-15}$ Pa^{-1} from experimental data obtained using a fretting wear test rig with a piezoelectric actuator. The contact pressure distributions and wear depths were also plotted along the contact surface in the three-dimensional finite element analysis. The results of the analyses showed a donut-shaped wear scar along the contacting boundary, which is a typical feature of fretting wear.

The results of this study can be applied to the prediction of fretting wear behavior at the steam generator tubes or the fuel rods in a nuclear power plant; hence, this study will provide information useful for the design of future steam generators and fuel rods.

2. FINITE ELEMENT ANALYSIS OF TWO-DIMENSIONAL FRETTING WEAR PROBLEMS

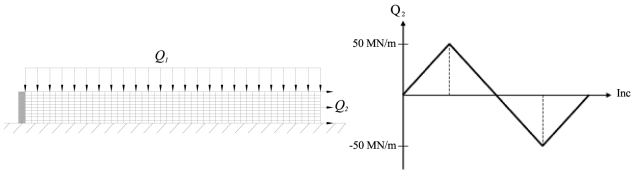

Fig. 1. Elastic Beam Subjected to Line Loads

A two-dimensional elastic beam problem with existing solutions by Strömberg [18] was chosen to demonstrate the feasibility of finite element analysis of the two-dimensional fretting wear problem. Figure 1 shows a 5×0.5 cm^2 elastic beam fixed at the left end and constrained to a rigid support at the bottom, with zero initial gap. The beam is subjected to a line load where Q_1 is fixed at 50 MN/m and Q_2 varies according to the history scheme between ± 50 MN/m, as shown in Fig. 1. Plane strain conditions with four-node bilinear finite elements were used in the analysis. The elastic beam is discretized by 50×10 finite elements and the number of increments during one load path is 50. The finite element analysis parameters in the analysis were assumed as follows: modulus of elasticity E = 210 GPa, Poisson's ratio ν = 0.3, friction coefficient μ = 0.2, and wear constant K=1.0 $\times 10^{-11}$ Pa^{-1}.

From the work rate model, the wear depth was defined as follows:

$$\text{wear depth} \equiv K \cdot u_t \cdot \sigma_n \tag{3}$$

where K is the wear constant, u_t is the relative slip defined as the difference between tangential displacements, and σ_n is the normal contact stress. In the first cycle, after calculating the stress and displacement fields of each node and element in the two-dimensional elastic finite element analysis, the wear depth was computed by applying the work rate model. After the first cycle, the finite element mesh was moved a distance equal to the amount of the wear depth and was therefore ready for the next cycle, and so forth.

The results of the analyses for the number of cycles, up to N =1000, are shown in Fig. 2. The evolution of fretting wear is illustrated by the distributions of wear depths along the contact surfaces as the number of cycles increases in Fig. 2. The result shows that wear depth increases with the number of cycles. The region bounded by $0 \le x \le 2$cm is interpreted as the stick region, the other region is considered as the slip region. Distributions of the normal contact pressure along the contact surface with increasing number of cycles are also sketched in Fig. 2, where large contact pressures are developed at the

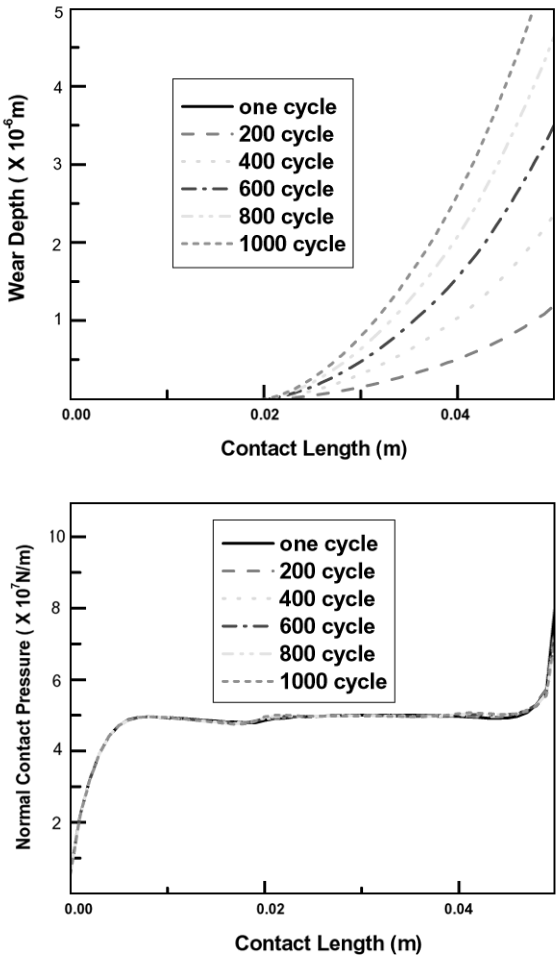

Fig. 2. Distributions of Wear Depth and Normal Contact Pressures up to N = 1000 cycles

end of the boundary.

In order to reduce the computation time required for the analysis, the concept of a control parameter *s* was introduced, which scaled up the wear constant and scaled down the actual number of cycles in the analysis. The effective wear constant $K_e(\equiv K\cdot s)$ and the effective number of analysis cycles $N_e(\equiv \frac{N}{s})$ were defined as the values of the wear constant and the number of analysis cycles increased by *s* times, respectively. Although the wear constant was $K = 1.0\times 10^{-11} Pa^{-1}$ in the computations, the effective wear constant $K_e(\equiv K\cdot s)$ was used in the actual analysis over the actual numbers of analysis cycles $N(\equiv N_e\cdot s)$, which had the same effect as analyzing the effective number of cycles N_e. The feasibility of introducing the control parameter *s* can be demonstrated by verifying that the results of different analyses are the same for different values of *s*.

To demonstrate the feasibility of parameter *s*, the results of analyses for different values, *s* =1, 10, 50, and 100, are compared in Fig. 3. The distributions of the wear depths and the normal contact pressures for the final cycles (*N*=1000) using different values of *s* are plotted in Fig. 3, which shows unstable results for especially large *s* values. Nevertheless, similar results were obtained for *s* =10; therefore, using this method provides a great advantage by reducing the analysis time required to obtain a reasonable solution.

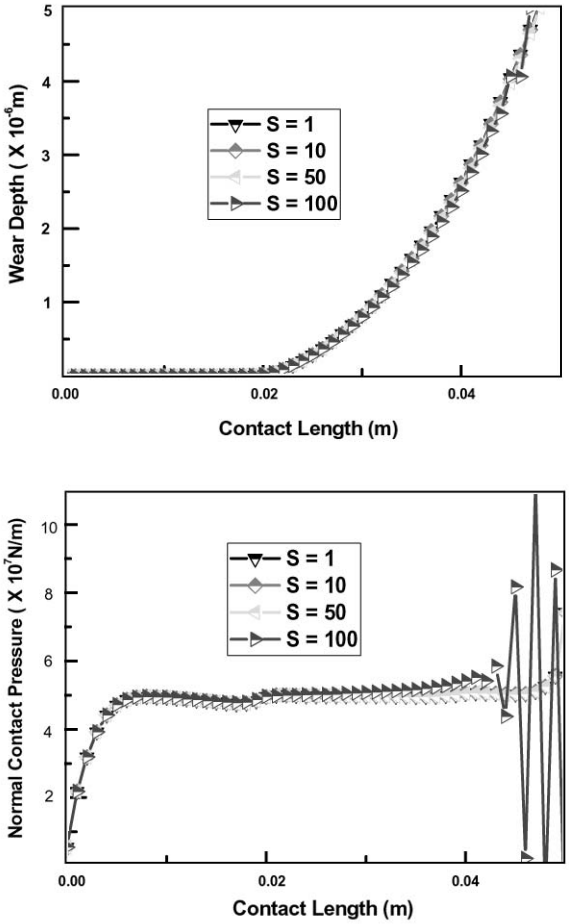

Fig. 3. Comparisons of Results for Different Levels of the Parameter *s*

Another way of demonstrating the feasibility of this methodology is to compare the results with the previous solutions by Strömberg [18], which are depicted in Fig. 4. Comparisons of the evolution of the fretting wear, indicated by the wear depth distributions along the contact surfaces as the number of cycles increases, are shown in Fig. 4. The normal contact pressure distributions along the contact surface as the number of cycles increases are also compared in Fig. 4. Qualitatively speaking, the results indicated similar behaviors; however, a quantitative comparison revealed a slight difference between the solutions. The difference is largely due to the location of stick-slip boundary. This quantitative difference might

be caused by the restrictive use of solution meshes in the numerical procedure after the theoretical formulation by Strömberg [18]. The results of the analyses behaved in a similar qualitative manner with the previous solutions by Strömberg [18].

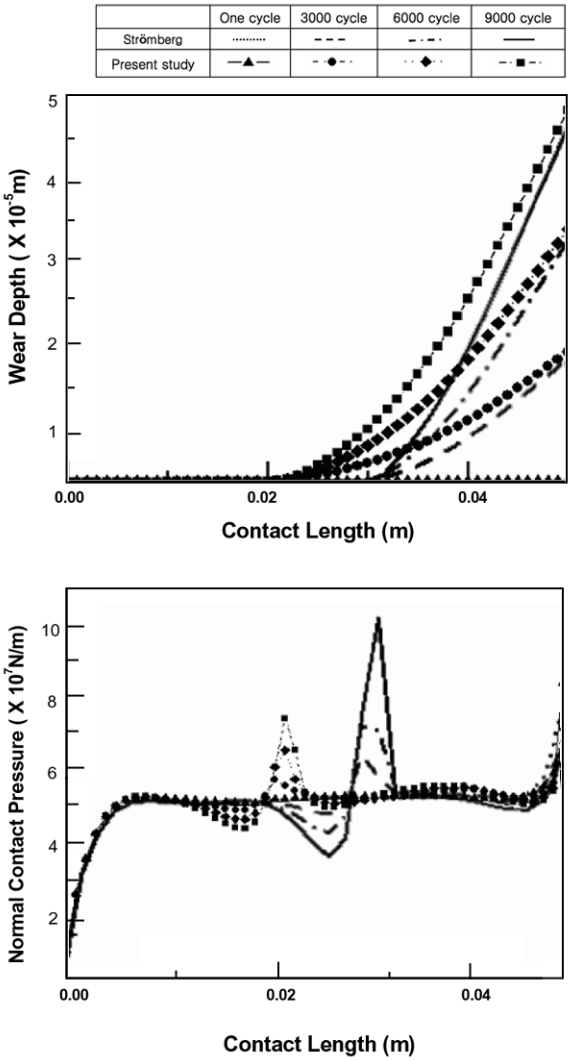

Fig. 4. Comparisons of the Results with the Solution by Strömberg

3. FINITE ELEMENT ANALYSIS OF THREE-DIMENSIONAL TUBE-TO-TUBE FRETTING WEAR PROBLEMS

In the three-dimensional finite element analysis, which simulated the actual tube-to-tube fretting wear tests, the model considered two Inconel tubes contacting at right angles, as shown in Fig. 5. The Inconel tube specimen had a diameter of 19 mm, thickness of 1 mm, and length of 35 mm. A quarterly symmetric three-dimensional finite element model was used, as shown in Fig. 5, with

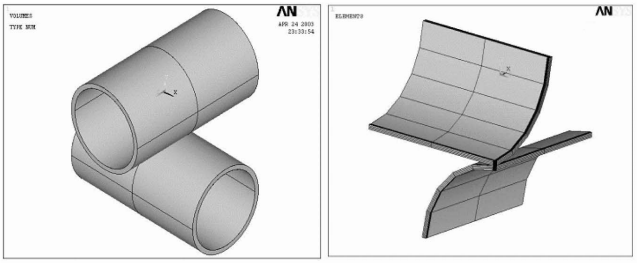

Fig. 5. Three-Dimensional Actual Model and Finite Element Model for Fretting Wear Tests

eight-node quadrilateral brick elements.

Since a steep stress distribution gradient was expected around the contact region, the size of the finite element mesh around the contact region was dealt with separately from the global region. In the three-dimensional finite element analysis, the fine mesh around the contact region resulted in a total of 12800 elements and 40512 nodes. A static loading of 70 *N*, equivalent to a pressure of 1 *MPa* in the contact area, was applied to the upper specimen in the vertical direction. The amplitude of the fretting wear was set to 100 μm, which was also the value used in the experiments. Compared to the two-dimensional finite element analysis, considerably longer computational times were expected in the three-dimensional analysis.

After demonstrating the feasibility of the two-dimensional finite element analysis algorithm, the method was extended to the three-dimensional problem shown in Fig. 5 to simulate actual experiments of the tube-to-tube fretting wear that occurs on the secondary side of the steam generator in a nuclear power plant. Figure 6 shows a photo and a schematic of a test rig with a piezoelectric actuator that was developed in the experimental phase of the fretting behavior analysis of an Inconel 690 tube. In comparison with traditional mechanically driven fretting wear testers, a test rig with a piezoelectric actuator has fine control within an order of 1 μm resolution, high stiffness, quick response, and so forth. From the experiments, the wear constant for the Inconel 690 tube in the work rate model was found to be K=26.7 $\times 10^{-15}$ Pa^{-1}, which was also used in the input data for the three-dimensional finite element analysis.

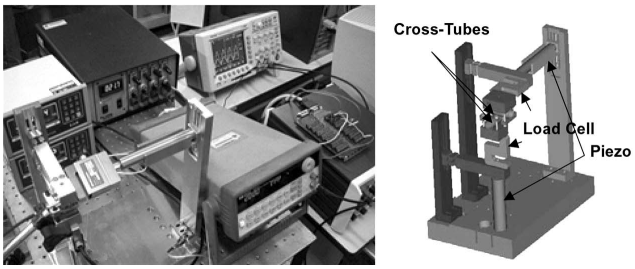

Fig. 6. Fretting Wear Test Rig with Piezoelectric Actuator

In the two-dimensional finite element analysis algorithm, the wear depth was computed by applying the work rate model to each cycle. The finite element mesh was then moved a distance equal to the amount of the wear depth for the next cycle. In three-dimensional finite element analyses of contact and wear problems, special care must be directed to the convergence, owing to the instability of the numerical solution.

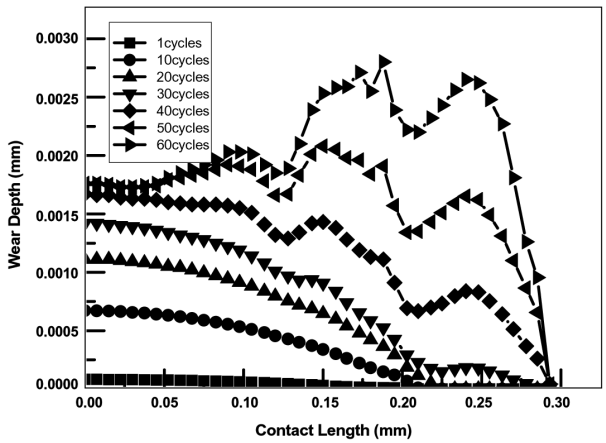

Fig. 7. Wear Depth Distributions along the Contact Surface as the Number of Cycles increases in the Fretting Wear Simulation (s = 40)

The results of the three-dimensional finite element analysis for a static loading of 70 *N* indicated that the half width of the contact region was 0.3 mm. The evolution of the fretting wear, indicated by the wear depth distributions along the contact surface of the Inconel 690 tube as the number of cycles increases, is depicted in Fig. 7 for parameter s =40 (K=1.07 $\times 10^{-12}$ Pa^{-1}). The size of the contact region increases with the number of cycles, and donut-shaped wear patterns appear as the number of cycles approaches the final stages of the simulation. Although the global wear shapes differ from those obtained in the two-dimensional cases, the results show the typical types of fretting wear patterns. Figure 8 shows the normal contact pressure distributions along the contact surface as the number of cycles increases.

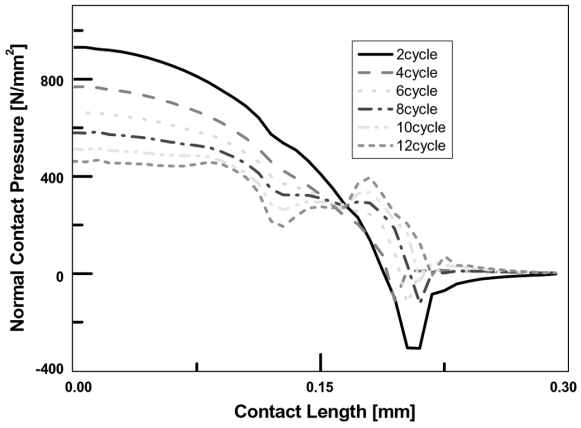

Fig. 8. Normal Contact Pressure Distributions along the Contact Surface as the Number of Cycles increases in the Fretting Wear Simulation (s = 40)

After the three-dimensional finite element analysis was completed, the wear profiles (s =40 after 40 cycles) for the entire contact area were collected and plotted in Fig. 9 using a three-dimensional graphic technique so that they could be compared with the wear amounts and wear profiles obtained from the experiments. Although quantitative comparisons with the experimental results were limited, owing to the difficulty of experimentally measuring the wear depth, parameters such as the fretting wear area and wear patterns were qualitatively similar.

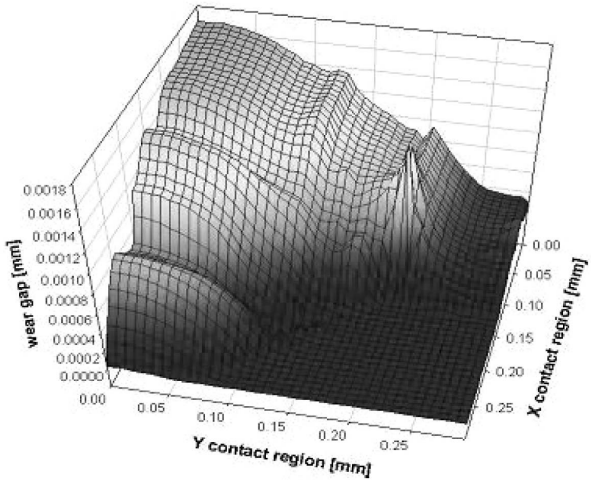

Fig. 9. Three-Dimensional Graphical Representation of the Wear Amount (s = 40 after 40 cycles)

4. CONCLUSIONS

The purpose of this study was to develop a finite element model that could numerically simulate fretting wear problems. Two-dimensional and three-dimensional finite element analyses were carried out to investigate the fretting wear behavior. The two-dimensional finite element analysis was used to simulate the frictional contact wear problem between an elastic beam and a rigid foundation. A comparison of the numerical results with the solutions by Strömberg [18] demonstrated the feasibility of introducing a control parameter *s*, which scaled up the wear constant and scaled down the cycle numbers. The two-dimensional finite element model was extended to three dimensions to simulate actual tube-to-tube fretting wear experiments. During the analysis,

donut-shaped wear patterns were observed as the number of cycles approached the final stages of the simulation. Wear profiles along the entire contact area were plotted using a three-dimensional graphic technique.

Acknowledgement

This study was supported by the Korean Institute of Science and Technology Evaluation and Planning (KISTEP) and by the Ministry of Science & Technology (MOST), Republic of Korea, through its National Nuclear Technology Program.

REFERENCES

[1] P. J. Blau, *et al., ASM Handbook - Friction, Lubrication and Wear Technology*, **18**, p. 242 (1995).
[2] E. M. Eden, W. N. Rose, and F. L. Cunningham, "Endurance of Metals," *Proc. Inst. Mech. Eng*., **4**, p. 839 (1911).
[3] G. A. Tomlinson, "The Rusting of Steel Surfaces in Strength," *Proc. R. Soc.* London, **A115**, p. 472 (1927).
[4] R. B. Waterhouse, "Fretting Corrosion," Pergamon, Oxford (1972).
[5] R. B. Waterhouse, *Fretting Fatigue*, Applied Science, London (1981).
[6] I. M. Feng, and H. H. Uhlig, "Fretting Corrosion of Mild Steel in Air and Nitrogen," *J. Appl. Mech*., **21**, p. 354 (1954).
[7] A. W. de Gee, C. P. L. Commissaris, and J. H. Zaat, "The Wear of Sintered Aluminum Powder (SAP) under Directions of Vibrational Contact," *Wear*, **7**, p. 535 (1964).
[8] P. L. Ko, "Experimental Studies of Tube Fretting in S/G and Heat Exchange," *Journal of Pressure Vessel Technology*, **101**, p. 125 (1979).
[9] O. Vingsbo, and S. Söderberg, "Fretting Maps", *Wear*, **126**, p. 131 (1988).
[10] N. J. Fisher, A. B. Chow, and M. K. Weckwerth, "Experimental Fretting Wear Studies of Steam Generator Materials", *Journal of Pressure Vessel Technology*, **117**, p. 312 (1995).
[11] F. M. Guerout, N. J. Fisher, D. A. Grandison, and M. K. Weckwerth, "Effect of Temperature on Steam Generator Fretting Wear", *ASME PVP*, **328**, p. 233 (1996).
[12] K. H. Cho, T. H. Kim, and S. S. Kim, "Fretting Wear Characteristics of Zircaloy-4 Tube", *Wear*, **219**, p. 3 (1998).
[13] D. G. Kim, and Y. Z. Lee, "Experimental Investigation in Sliding and Fretting Wear of Steam Generator Tube Materials", *Wear*, **250**, p. 673 (2001).
[14] H. K. Kim, S. J. Kim, K. H. Yoon, H. S. Kang, and K. N. Song, "Fretting Wear of Laterally Supported Tube", *Wear*, **250**, p. 535 (2001).
[15] Y. H. Lee, H. K. Kim, H. D. Kim, C. Y. Park, and I. S. Kim, "A Comparative Study on the Fretting Wear of Steam Generator Tubes in Korean Power Plants", *Wear*, **255**, p. 1198 (2003)
[16] J. K. Hong, and I. S. Kim, "Environment Effects on the Reciprocating Wear of Inconel 690 Steam Generator Tubes", *Wear*, 255, p. 1174 (2003).
[17] T. J. Mackin, J. Yang, and D. Warren, "Influence of Fiber Roughness on the Sliding Behavior of Sapphire Fiber and metrics", *J. Am. Ceram. Soc*., **75**, p. 3358 (1992).
[18] N. Strömberg, "An Augmented Lagrangian Method for Fretting Problem", *Eur. J. Mech. A/Solid*, **16**, p. 573 (1997).
[19] N. P. Suh, *Tribophysics*, Prentice-Hall Inc., Englewood Cliffs, NJ. (1986)